

# Encoding qubits into harmonic-oscillator modes via quantum walks in phase space

Wang-Chang Su, Chai-Yu Lin, and Shin-Tza Wu\*

Department of Physics, National Chung Cheng University, Chiayi 621, Taiwan

(Dated: June 27, 2022)

We propose linear optical schemes for encoding arbitrary logical states of a quantum bit (qubit) into a harmonic oscillator mode, which was originally put forward by Gottesman, Kitaev, and Preskill (GKP) [Phys. Rev. A **64**, 012310 (2001)]. Starting with a squeezed-vacuum state with an arbitrary polarization, we show that a linear-optical setup that implements quantum walks of the state in phase space is capable of generating an output state that corresponds to a variant of the GKP codeword states. In particular, with a coin toss that projects the mode polarization onto the diagonal direction, we show that the resulting *dissipative* quantum walks can generate qubit encoding akin to the prototypical GKP encoding. We analyze the performance of our codewords for error corrections and find that even without optimization our codewords outperform the GKP ones by a narrow margin. This demonstrates the potential of the proposed encoding scheme.

## I. INTRODUCTION

Computing based on quantum mechanical principles (i.e., quantum computing) requires exquisite control of quantum systems [1]. Thanks to advancements in experimental techniques, tremendous progress has been made for achieving this goal during the past few years [2]. For large scale quantum computing, it is indispensable to have an architecture that enables efficient detection and correction of errors during the computation [3]. Recently, there has been significant progress towards this direction in the field of continuous-variable (CV) measurement-based quantum computing, which seeks to achieve quantum computing by sequence of adaptive measurements over highly entangled resource states in a state space with continuous spectrum [4, 5]. In particular, Menicucci has shown that fault-tolerant quantum computing can be achieved in this scheme provided resource states with squeezing above 20.5 dB are available [6]. Recently, with the aid of topological codes, this squeezing threshold has been reduced to less than 10 dB [7, 8]. Essential to these breakthroughs is a quantum error-correcting scheme due to Gottesman, Kitaev, and Preskill (GKP) [9]. In this approach, quantum information is encoded through a “hybrid” quantum bit (qubit) embedded in the (quantum mechanical) phase space of a quantum harmonic oscillator. Despite the importance of the GKP scheme, existing proposals for the experimental generation of GKP qubits remain to pose major challenges [10–17] (see, however, the recent report in Ref. 18). In this paper we propose a new scheme for preparing GKP qubits through quantum walks (QWs) of an oscillator mode in phase space [19, 20]. Although our scheme should be generalizable to other systems, we will focus mainly on optical systems in the following.

In the CV approach to quantum computing, quantum information are carried by quantum modes (aka “qumodes”) with the logical states encoded via eigenstates of the canonical coordinates of the field mode,

which are usually likened to the position and momentum of a harmonic oscillator [21, 22]. Decoherence of the qumode then manifests as shift errors in these basis states. In order to correct such errors, GKP propose to invoke “hybrid” qubits that consist of superpositions of uniformly spaced position eigenstates separated by  $2\sqrt{\pi}$  [9]

$$|0\rangle_L = \sum_{s=-\infty}^{\infty} |2s\sqrt{\pi}\rangle_x = \frac{1}{\sqrt{2}} \sum_{s=-\infty}^{\infty} |s\sqrt{\pi}\rangle_p, \\ |1\rangle_L = \sum_{s=-\infty}^{\infty} |(2s+1)\sqrt{\pi}\rangle_x = \frac{1}{\sqrt{2}} \sum_{s=-\infty}^{\infty} (-1)^s |s\sqrt{\pi}\rangle_p, \quad (1)$$

where  $|x\rangle_x$  and  $|p\rangle_p$  are, respectively, position and momentum eigenstates. Thus the position-space wavefunctions for the codewords  $|0\rangle_L$  and  $|1\rangle_L$  comprise combs of delta functions located at, respectively, even and odd multiples of  $\sqrt{\pi}$ . In the presence of shift errors, it is then possible to correct sufficiently small errors in the encoded qubits through position and momentum measurements [9]. However, the GKP codeword states (1) require infinite squeezing, and hence infinite energy. In practice, therefore, one must approximate (1) through finitely squeezed states, such as uniformly spaced Gaussian spikes modulated by Gaussian envelopes [9]

$${}_x\langle x|\tilde{l}\rangle_L \propto \sum_n' e^{-\frac{n^2\pi\Delta_p^2}{2}} \exp\left[-\frac{(x-n\sqrt{\pi})^2}{2\Delta_x^2}\right], \\ {}_p\langle p|\tilde{l}\rangle_L \propto \sum_n (-1)^{nl} e^{-\frac{\Delta_x^2 p^2}{2}} \exp\left[-\frac{(p-n\sqrt{\pi})^2}{2\Delta_p^2}\right], \quad (2)$$

where  $l = \{0, 1\}$  are the logical bit values,  $\sum_n'$  in the position-space wavefunctions indicate summations over even/odd integers  $n$  for  $l = 0/1$ , and  $\Delta_x$ ,  $\Delta_p$  are the widths of the Gaussians. It is our goal in the present paper to provide experimentally feasible schemes for generating approximate GKP codewords such as (2) by implementing QWs in phase space for an optical mode through adapting the setup of Schreiber *et. al.* [23] to our case. In contrast to its classical counterpart, QW takes place

\* phystw@gmail.com

in accordance with a quantum coin that admits superpositions of orthogonal coin states [19, 20]. By taking the polarization of a squeezed coherent state as the “coin” configuration, we will show that GKP-type codewords can be generated through QWs of the state under appropriate “coin-toss rules”. As we will show, by changing the nature of the coin toss, one can attain GKP-type encodings with different characteristics. Our approach thus offers not only a promising pathway to the generation of GKP qubits, but also opens up new dimensions to the GKP encoding.

In the following, we shall start in Sec. II by first illustrating a linear-optical setup that implements QWs in phase space for an optical mode. We will then explain how this design can be applied to transcribe the polarization configuration of a squeezed vacuum state into the logical state of a GKP qubit. We will illustrate two instances for the encoding: One involving generic unitary QWs, while the other *dissipative*, non-unitary QWs. Performance of our encoding scheme for the dissipative case will then be analyzed. Finally, we conclude in Sec. III with a summary and brief discussions for our findings. For presentational clarity, we relegate some details to the Appendices.

## II. FROM QUANTUM WALKS TO THE GKP ENCODING

Let us consider an implementation for one-dimensional QWs in phase space for an optical mode through the setup illustrated in Fig. 1(a), which is an adaptation of the original design due to Schreiber *et. al.* [23]. Suppose here the optical mode has the mode operator  $\hat{a} = (\hat{x} + i\hat{p})/\sqrt{2}$ , where  $\hat{x}$  and  $\hat{p}$  are, respectively, the “position” and “momentum” quadrature operators of the qumode. From the commutation relation  $[\hat{a}, \hat{a}^\dagger] = 1$  for the mode operators, it follows that  $[\hat{x}, \hat{p}] = i$ , which corresponds to setting  $\hbar = 1$  for us. For the QW, we will be concerned with position-squeezed states with definite polarizations, which will be denoted as  $|q\rangle_r|\epsilon\rangle$ . Here the subscript  $r$  indicates the squeezing parameter,  $q$  is the expectation value  $\langle\hat{x}\rangle$  of the state in units of  $\sqrt{2}$  times the QW step length  $\Delta\xi$  [24], and  $\epsilon$  represents polarization along, e.g., horizontal ( $H$ ) and vertical ( $V$ ) directions. More precisely, in terms of the phase-space displacement operator  $\hat{D}(\xi) \equiv \exp\{\xi(\hat{a}^\dagger - \hat{a})\}$  for real  $\xi$  and the squeezing operator  $\hat{S}(r) \equiv \exp\{\frac{r}{2}(\hat{a}^2 - \hat{a}^{\dagger 2})\}$  for real  $r$ , we will be considering squeezed coherent states

$$|q\rangle_r \equiv \hat{D}(q\Delta\xi) \hat{S}(r) |\text{vac.}\rangle \quad (3)$$

with  $|\text{vac.}\rangle$  the vacuum state of the qumode. Therefore, in the language of QW, the state  $|q\rangle_r|\epsilon\rangle$  corresponds to a walker at position  $q \times \sqrt{2}\Delta\xi \equiv q\Delta x$  with a “coin configuration”  $\epsilon$  [24].

To see how the design in Fig. 1(a) implements QWs in phase space for our qumode, let us consider an input state  $|\psi\rangle$  entering the setup. The half-wave plate (HWP)

oriented at an angle  $22.5^\circ$  relative to the horizontal axis induces the following transformation in the polarization basis  $\{|H\rangle, |V\rangle\}$

$$\hat{C}_H = \frac{1}{\sqrt{2}} \begin{pmatrix} 1 & 1 \\ 1 & -1 \end{pmatrix}, \quad (4)$$

which corresponds to a Hadamard coin-toss for the QW [20, 23]. The polarization beamsplitter (PBS) subsequently diverts the two polarization components into different paths along which the  $H$  and the  $V$  components of the qumode are displaced, respectively, by  $\pm\Delta\xi$  in phase space via amplitude and phase modulations [25]. This corresponds to the action of a translation operator  $\hat{T}$  whose operation is conditioned to the coin configuration (i.e. polarization) of the qumode

$$\hat{T}(\Delta\xi) = \hat{D}(+\Delta\xi) \otimes |H\rangle\langle H| + \hat{D}(-\Delta\xi) \otimes |V\rangle\langle V|. \quad (5)$$

The two components are then combined at a second PBS and result in the final state  $\hat{W}|\psi\rangle$ , where the “walk operator”  $\hat{W}$  describes the overall action of the setup in Fig. 1(a), namely

$$\hat{W} = \hat{T}(\Delta\xi) \left( \hat{I} \otimes \hat{C}_H \right) \quad (6)$$

with  $\hat{I}$  the identity operator. Thus we see that the setup has implemented one single step of QW in phase space for the qumode.

We shall now explain how the design above can help prepare GKP qubits in an experimentally feasible way. To this end, we will consider a position-squeezed vacuum state polarized in an arbitrary direction

$$|\psi_{\text{in}}\rangle = |0\rangle_r (\alpha|H\rangle + \beta|V\rangle), \quad (7)$$

where  $|\alpha|^2 + |\beta|^2 = 1$ . As we will demonstrate in the following, by means of the QW implementation above, one can transcribe the “logical state” imprinted in the mode polarization onto the “coordinate” degrees of freedom  $\{|q\rangle_r\}$  of the qumode through QWs. Since distinct coin-toss transformations can lead to rather different walk patterns in the QWs [19, 20], it can be anticipated that different encodings can be achieved through different coin-toss transformations. In the following, we will first consider the case of the Hadamard coin-toss (4), which induces unitary evolution of the input state (7). As we shall find out, the consequent codewords will be quite different from the approximate GKP codewords in (2). We will then turn to another coin-toss transformation, which will engender codeword states that are similar to the “standard” ones in (2).

### A. Generic (unitary) quantum-walk encoding

For a walker that localizes initially at the origin, after even (odd) steps of QWs the wavefunction of the walker would become coherent superpositions of localized states over even (odd) multiples of the step length. In view of

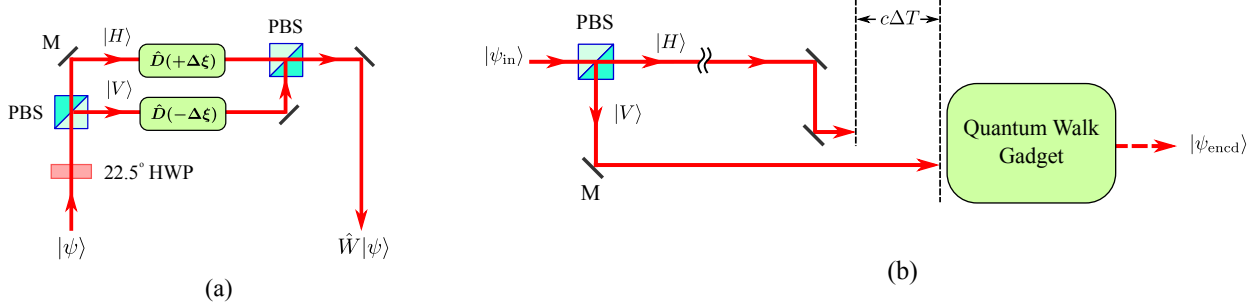


FIG. 1. (a) Schematics for a setup that implements QWs in the phase space of an optical mode. Here the 22.5° half-wave plate (HWP) furnishes a Hadamard coin-toss for QWs. The polarization beamsplitter (PBS) transmits optical modes with horizontal ( $H$ ) polarization and reflects those with vertical ( $V$ ) polarization.  $\hat{D}(\pm\Delta\xi)$  are displacement operators that shift the optical mode by  $\pm\Delta\xi$  in phase space. A set of mirrors (M's) are used to direct the propagation of the qumode. As explained in the text, an input state  $|\psi\rangle$  takes one step of QW after passing through the setup and becomes  $\hat{W}|\psi\rangle$  at the output. (b) Schematics for our GKP encoding scheme. The PBS splits the two polarization components of the input state  $|\psi_{\text{in}}\rangle$ . The  $H$  component is then delayed in time by  $\Delta T$  behind the  $V$  component with  $\Delta T$  the time duration for one single step of QW. The two beams are guided into a QW-gadget that implements QWs based on the design of (a). Upon output, the beams are recombined to yield the encoded state  $|\psi_{\text{encd}}\rangle$ . Here  $c$  stands for the speed of light.

the structure of the ideal GKP codewords (1), it is clear that this feature of QWs can be exploited to prepare GKP qubits. Let us suppose the availability of a QW-gadget, which is built based on the design of Fig. 1(a) and is capable of controlling the number of steps of QWs taken by an input state [i.e., the number of loops passing the setup of Fig. 1(a) inside the gadget]. If each single step of QWs takes time  $\Delta T$  inside the gadget, for the input state (7) suppose we separate the  $H$  and the  $V$  components of the polarization using a PBS, and subsequently delay, say, the  $H$  component by time  $\Delta T$  behind the  $V$  component [see Fig. 1(b)]. Then when the  $H$  component enters the QW-gadget, the  $V$  component would have completed exactly one step of QWs. Therefore, at the output of the QW-gadget, where the two components are recombined, the original  $H$  component would be exactly one step behind the original  $V$  component in the QW. Thus the two components will be distributed over sites of opposite parities, and a GKP-type encoding is then furnished for the input state (7) via the architecture of Fig. 1(b).

More precisely, suppose the initial state (7) is sent into the setup of Fig. 1(b) so that its  $H$  and  $V$  components would complete, respectively,  $N$  and  $(N+1)$  steps of QWs when leaving the QW-gadget. One would then have the output state

$$|\psi_{\text{out}}\rangle = \alpha|\psi_N^{(H)}\rangle + \beta|\psi_{N+1}^{(V)}\rangle, \quad (8)$$

where  $|\psi_N^{(\epsilon)}\rangle$  are the state vectors for an initial state  $|0\rangle_r|\epsilon\rangle$  with polarization  $\epsilon = \{H, V\}$  after  $N$  steps of QWs. One can find analytically that [26]

$$|\psi_N^{(\epsilon)}\rangle = \sum_{n=-N}^N' |n\rangle_r \left( u_N^{(\epsilon)}(n)|H\rangle + v_N^{(\epsilon)}(n)|V\rangle \right), \quad (9)$$

where  $\sum_n'$  indicates summation over every other integers, i.e.  $n = \{-N, -(N-2), \dots, (N-2), N\}$ . To avoid distractions, we supply explicit expressions for the amplitudes  $u_N^{(\epsilon)}(n)$  and  $v_N^{(\epsilon)}(n)$  in Appendix A 1. Clearly, for instance, if  $N$  is even,  $|\psi_N^{(H)}\rangle$  in (8) would cover only even sites  $n$ , while  $|\psi_{N+1}^{(V)}\rangle$  only odd sites  $n$ . By defining the encoded logical basis states here

$$|0\rangle_{\text{QW}} \equiv |\psi_N^{(H)}\rangle \quad \text{and} \quad |1\rangle_{\text{QW}} \equiv |\psi_{N+1}^{(V)}\rangle, \quad (10)$$

we then have from (8) the encoded state for the input state (7)

$$|\psi_{\text{encd}}\rangle = \alpha|0\rangle_{\text{QW}} + \beta|1\rangle_{\text{QW}}. \quad (11)$$

Our setup in Fig. 1(b) can thus furnish GKP-type encoding for any arbitrary input states.

To find the position-space and the momentum-space wavefunctions for the codewords  $|0\rangle_{\text{QW}}$  and  $|1\rangle_{\text{QW}}$ , we note that from (3) one can obtain the wavefunctions for the squeezed coherent states  $|n\rangle_r$  in the general formula (9)

$$\begin{aligned} {}_x\langle x|n\rangle_r &= \frac{e^{+\frac{r}{2}}}{\pi^{\frac{1}{4}}} \exp\left[\frac{-(x-n\Delta x)^2}{2e^{-2r}}\right], \\ {}_p\langle p|n\rangle_r &= \frac{e^{-\frac{r}{2}}}{\pi^{\frac{1}{4}}} \exp\left[+inp\Delta x - \frac{p^2}{2e^{+2r}}\right], \end{aligned} \quad (12)$$

where  $\Delta x \equiv \sqrt{2}\Delta\xi$  as before [24]. Making use of (12), one can obtain the wavefunctions for the codeword states  $|0\rangle_{\text{QW}} = |\psi_N^{(H)}\rangle$  and  $|1\rangle_{\text{QW}} = |\psi_{N+1}^{(V)}\rangle$  using (9) and the expressions for the amplitudes  $u_N^{(\epsilon)}$ ,  $v_N^{(\epsilon)}$ , and etc. from Appendix A 1. Setting  $\Delta x = \sqrt{\pi}$  for the QWs, we show in Fig. 2 the probability densities in position and momentum spaces for the QW codewords  $|0\rangle_{\text{QW}}$  and  $|1\rangle_{\text{QW}}$ , together with the conjugate states  $|+\rangle_{\text{QW}} \equiv$

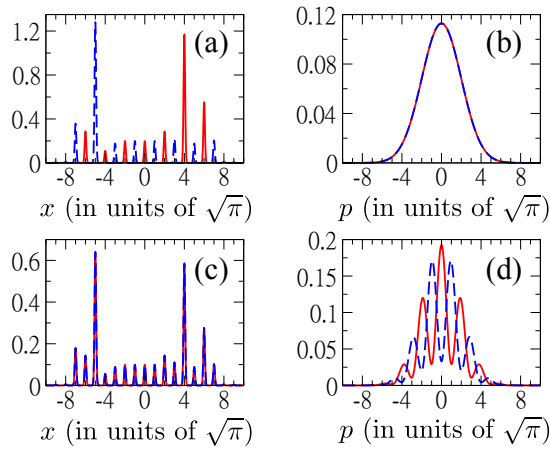


FIG. 2. Probability densities in position space and momentum space for generic QW codewords with  $N = 8$  at a squeezing with  $e^{-r} = 0.2$  ( $\sim 13.98$  dB). Panels (a) and (b) illustrate the results for  $|0\rangle_{\text{QW}}$  (solid curves) and  $|1\rangle_{\text{QW}}$  (dashed curves), while panels (c) and (d) show those for  $|+\rangle_{\text{QW}} \equiv (|0\rangle_{\text{QW}} + |1\rangle_{\text{QW}})/\sqrt{2}$  (solid curves) and  $|-\rangle_{\text{QW}} \equiv (|0\rangle_{\text{QW}} - |1\rangle_{\text{QW}})/\sqrt{2}$  (dashed curves).

$(|0\rangle_{\text{QW}} + |1\rangle_{\text{QW}})/\sqrt{2}$  and  $|-\rangle_{\text{QW}} \equiv (|0\rangle_{\text{QW}} - |1\rangle_{\text{QW}})/\sqrt{2}$  for the case of  $N = 8$  at a squeezing with  $e^{-r} = 0.2$  (corresponding to  $\sim 13.98$  dB squeezing).

From Fig. 2, we see that, despite the unusual envelopes, the probability densities of the QW codewords exhibit features characteristic of approximate GKP codewords that are essential for correcting shift errors [11]. In particular, the position distributions of the codewords  $|0\rangle_{\text{QW}}$  and  $|1\rangle_{\text{QW}}$  consist of Gaussian spikes at, respectively, even and odd multiples of  $\sqrt{\pi}$ , while the momentum distributions of the codewords  $|+\rangle_{\text{QW}}$  and  $|-\rangle_{\text{QW}}$  manifest peaks at, respectively, even and odd multiples of  $\sqrt{\pi}$ . Therefore, in principle, the QW codewords here can be adopted to correct shift errors in accordance with the GKP scheme, despite the issues with their performance and probably also efficiencies [6]. The key drawbacks of the QW codewords (10) reside in their momentum distributions, such as the featureless Gaussians in Fig. 2(b) for  $|0\rangle_{\text{QW}}$  and  $|1\rangle_{\text{QW}}$ , and the broad peaks in Fig. 2(d) for  $|+\rangle_{\text{QW}}$  and  $|-\rangle_{\text{QW}}$ , which would render the correction for  $p$ -errors ineffective. We find numerically that these features are independent of the QW steps  $N$ , likely due to unitarity of the QWs here. Since different coin-toss transformations for QWs can lead to very different walk patterns [19, 20], one possible remedy for the present dilemma is to replace the coin-toss operation (4) with a new one, say, by adjusting the angle of the HWP in Fig. 1(a). Alternatively, since the difficulty with the codewords  $|0\rangle_{\text{QW}}$  and  $|1\rangle_{\text{QW}}$  lies in the lack of (polarization independent) structures in their momentum distributions, one can attempt to implement periodic structures in both position and momentum directions through two-dimensional QWs [27]. As our point

here is to demonstrate the feasibility of the setups in Fig. 1 for generating GKP-type encodings in a generic setting, we shall not pursue these issues further. However, in view of the “unconventional” profiles in the probability densities of the QW codewords in Fig. 2, it is natural to ask whether our scheme is capable of producing QW codewords akin to the “standard” GKP ones as in (2). As we will now show, with appropriate coin-toss transformation, this is indeed possible.

## B. Dissipative (non-unitary) quantum-walk encoding

In order to generate QWs with Gaussian probability distributions, intuitively one might expect decoherence of the state must be incorporated, so that the QWs would become classical and yield the desired probability distributions [28]. However, this would inevitably lead to mixed states, which are unfavorable for our purposes here, as the codeword states must be pure states. To find the way out, we note that the nonclassical nature of the QWs arises from the interference between the coin-toss results associated with the  $H$  and the  $V$  components. Therefore, if we project the state vector at each step of the QWs, so that the two polarization components won’t interfere, it would then be possible to generate coherent superpositions of “classically” distributed Gaussian spikes. In other words, by “resetting” the coin state of the walker to a symmetric combination of the  $H$  and the  $V$  polarizations in each step of the QWs, one can then generate the desired walk pattern. It thus follows that one should replace the coin-toss transformation (4) with the projection operator for the diagonal polarization  $|D\rangle = (|H\rangle + |V\rangle)/\sqrt{2}$ , i.e.

$$\hat{C}_D = |D\rangle\langle D| = \frac{1}{2} \begin{pmatrix} 1 & 1 \\ 1 & 1 \end{pmatrix}. \quad (13)$$

With this change, as we shall show below, we are then able to achieve the targeted codeword states. For the setups in Fig. 1, we now have to modify by replacing the HWP with a polarizer for the  $D$  polarization, which induces exactly the transformation (13). Since the projection operator would reduce the total probability, the QWs here become nonunitary, and we shall refer to them as “dissipative” ones.

For the setups of Fig. 1 modified with the new coin-toss operation (13), the calculation for the new encoded states proceeds in exactly the same manner as before. After the  $H$  component and the  $V$  component of the input state (7) have completed, respectively,  $N$  and  $(N+1)$  steps of QWs, one can find an output state with the same structure as Eqs. (8) and (9), but now with different explicit forms for the amplitudes  $u_N^{(e)}(n)$  and  $v_N^{(e)}(n)$  (see Appendix A 2). At this point, it is tempting to conclude immediately that the encoding can now be achieved in exactly the same way as in (10). This is, however, incorrect because we now have nonunitary, dissipative QWs

and thus must take extra care for the normalization of the state vectors. Moreover, in order that the codeword states would resemble better the approximate GKP codewords (2), we find it advantageous to project the final states of the QWs onto the  $D$  polarization. Namely, at the output of the QW-gadget in Fig. 1(b), it is favorable to place a  $D$ -polarizer and project the encoded states onto the diagonal polarization  $|D\rangle$ . For the initial state  $|0\rangle_r|\epsilon\rangle$  the resulting *unnormalized* state vector after  $N$  steps of dissipative QWs (including the action of the  $D$ -polarizer at output) takes the form

$$|\psi_N\rangle = \sum_{n=-N}^N w_N(n) |n\rangle_r |D\rangle, \quad (14)$$

where

$$w_N(n) = \frac{1}{2^{N+\frac{1}{2}}} \binom{N}{\frac{N+n}{2}}. \quad (15)$$

Note that because the  $H$  and the  $V$  components are now symmetrical, we have dropped the superscript  $\epsilon$  for polarizations in (14) and (15). In terms of the normalized state vectors for (14)

$$|\phi_N\rangle \equiv Z_N^{-1/2} |\psi_N\rangle \quad (16)$$

with  $Z_N \equiv \langle \psi_N | \psi_N \rangle$ , we find the output state for the dissipative QWs

$$\begin{aligned} |\psi_{\text{out}}\rangle &= \alpha \sqrt{Z_N} |\phi_N\rangle + \beta \sqrt{Z_{N+1}} |\phi_{N+1}\rangle \\ &\propto \alpha' |\phi_N\rangle + \beta' |\phi_{N+1}\rangle, \end{aligned} \quad (17)$$

where we have denoted in the second line  $\alpha' \equiv \alpha/\sqrt{|\alpha|^2 + \gamma^2|\beta|^2}$  and  $\beta' \equiv \gamma\beta/\sqrt{|\alpha|^2 + \gamma^2|\beta|^2}$  with  $\gamma \equiv \sqrt{Z_{N+1}/Z_N}$ . Therefore, identifying

$$|0\rangle_{\text{dQW}} \equiv |\phi_N\rangle \quad \text{and} \quad |1\rangle_{\text{dQW}} \equiv |\phi_{N+1}\rangle, \quad (18)$$

we arrive at the following encoding for the input state (7)

$$|\psi_{\text{encd}}\rangle = \mathcal{N}(\alpha' |0\rangle_{\text{dQW}} + \beta' |1\rangle_{\text{dQW}}) \quad (19)$$

with  $\mathcal{N} \equiv \sqrt{|\alpha'|^2 Z_N + |\beta'|^2 Z_{N+1}}$ . Note that the coefficients  $\alpha, \beta$  in the original state (7) have been modified in the final encoding (19) due to the dissipative nature of the QWs. Therefore, when applying this encoding scheme, one must prepare the input state properly, so that the desired encoded states can be attained at the output.

To find the wavefunctions of the present codewords, one can again use (12) in (18) [together with Eqs. (14)–(16)]. For the momentum-space wavefunction, the summation over the site index  $n$  can be done analytically. We find

$${}_p \langle p | \phi_N \rangle = \left( \frac{e^{-r}}{2\sqrt{\pi} Z_N} \right)^{\frac{1}{2}} \exp \left[ -\frac{p^2}{2e^{+2r}} \right] \cos^N(p\Delta x) |D\rangle. \quad (20)$$

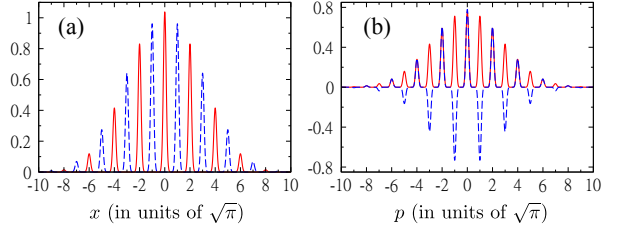


FIG. 3. (a) Position and (b) momentum wavefunctions for the dissipative QW codewords  $|0\rangle_{\text{dQW}}$  (solid curves) and  $|1\rangle_{\text{dQW}}$  (dashed curves) with  $N = 8$  at a squeezing with  $e^{-r} = 1/\sqrt{8\pi} \sim 0.199$  ( $\sim 14.00$  dB squeezing).

For the position-space wavefunction, it is of particular interest to examine its large  $N$  limit, for which the binomial distribution would tend to a Gaussian distribution. Applying Stirling's formula, we find for large  $N$

$${}_x \langle x | \phi_N \rangle \approx \left( \frac{2e^{+r}}{\pi \sqrt{N}} \right)^{\frac{1}{2}} \sum_{n=-N}^N e^{-\frac{n^2}{2N}} \exp \left[ -\frac{(x - n\Delta x)^2}{2e^{-2r}} \right] |D\rangle. \quad (21)$$

For the normalization in (21), we have taken the squeezed coherent states  $\{|n\rangle_r\}$  to be approximately orthonormal, so that  $Z_N$  in (16) can be approximated as

$$Z_N \approx \frac{1}{2^{2N+1}} \binom{2N}{N} \approx \frac{1}{2\sqrt{\pi N}}. \quad (22)$$

Taking  $\Delta x = \sqrt{\pi}$  in (21) and comparing the expression with the approximate GKP codewords (2), we see that in the large  $N$  limit the dissipative QW (or dQW, for short) codewords (18) correspond to approximate GKP codewords with width  $\Delta_x \approx e^{-r}$  and  $\Delta_p \approx 1/\sqrt{\pi N}$ . Therefore, for shift errors symmetric in the position and the momentum quadratures, following GKP [9], the choice for encodings with  $\Delta_x = \Delta_p$  becomes here  $e^{+r} = \sqrt{N\pi}$ . As an illustration, we plot in Fig. 3 the wavefunctions for the dQW codewords for the case with  $N = 8$  and  $e^{-r} = 1/\sqrt{8\pi} \sim 0.199$  (corresponding to  $\sim 14.00$  dB squeezing), which carry the hallmarks of approximate GKP codewords (2).

In order to evaluate the performance of the dQW codewords (18), we consider the error-correcting scheme of Ref. 29 and find the probability  $P_{\text{no error}}$  for repeated error corrections using the dQW codewords without incurring Pauli errors (see Appendix B for details). For this calculation, we consider  $N$ -step dQW encoding with width  $e^{-r} = 1/\sqrt{N\pi} \equiv \Delta$ . The results are shown in Fig. 4, where we also plot the results for the approximate GKP codewords (2) with  $\Delta_x = \Delta_p = \Delta$  for comparison. It is encouraging to find that the dQW codewords in fact outperform their GKP counterparts for all  $\Delta$  by a small margin. In particular, for the  $N = 8$  dQW codewords we get  $P_{\text{no error}} \simeq 0.936$  [vs.  $\simeq 0.929$  for the GKP case] at the squeezing  $\sim 14.00$  dB, which is within current experimental capabilities [30]. Although for dQW codewords

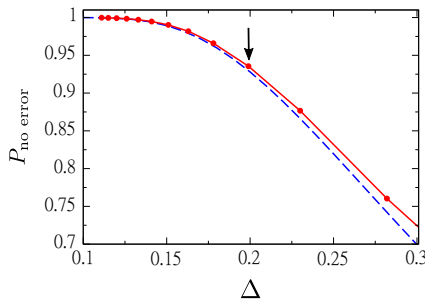


FIG. 4. The probability for repeated error corrections without Pauli errors using dissipative QW codeword  $|0\rangle_{dQW}$  (dots) with  $\Delta = e^{-r} = 1/\sqrt{N\pi}$ , where the solid line serves as guide to the eyes. For comparison, results for the approximate GKP codeword  $|\tilde{0}\rangle_L$  (dashed line) with  $\Delta_x = \Delta_p = \Delta$  are also shown. The arrow indicates the point for  $N = 8$  and  $\Delta = 1/\sqrt{8\pi} \sim 0.199$  (corresponding to  $\sim 14.0$  dB squeezing) in the dissipative QW codeword.

with  $N = 10$  one can even attain  $P_{\text{no error}} \simeq 0.966$  at a squeezing  $\sim 14.97$  dB, which lies barely below the 15 dB squeezing achieved in Ref. 30, performing 10 and 11 steps of QWs can be more challenging experimentally.

### III. CONCLUSION AND DISCUSSIONS

In summary, we have shown that by implementing QWs in phase space for an optical mode through linear-optical setups, it is possible to furnish GKP-type encodings for quantum error-corrections. In addition to

demonstrating an encoding through generic unitary QWs that produces codewords with “unconventional” profiles, we show further that an encoding via *dissipative*, nonunitary QWs can generate codeword states similar to the standard GKP ones. We examine the performance of the dissipative QW codewords for error corrections and find that they do better than the standard GKP codewords by a small amount. In view of this result, it is promising that with optimized coin-toss transformations, one may find QW codewords that perform even better. Our work thus not only offers possible experimental realizations for the GKP encoding, but also uncovers new avenues for its probable extensions.

Although we have focused on optical systems throughout this paper, one can envision possible generalizations of the QW-encoding scheme to other CV systems for which QWs can be implemented [20]. Moreover, our encoding scheme has been based on one-dimensional QWs, as pointed out earlier, its extensions to encodings with *two-dimensional* QWs [27] can be useful for rectifying the undesirable momentum distributions of the codewords in Fig. 2. At the same time, this may also help enhance the versatility of the QW-encoding scheme. In view of the multitude of walk patterns available for QWs [19, 20], the QW-encoding scheme proposed in the present paper thus opens up a new dimension for the GKP encoding that is yet to be explored.

We thank Prof. Dian-Jiun Han for useful discussions. This research is supported by the Ministry of Science and Technology of Taiwan through grant MOST 107-2112-M-194-002.

### Appendix A: Formulas for the amplitudes $u_N^{(\epsilon)}(n)$ and $v_N^{(\epsilon)}(n)$ for the codeword states

We provide here explicit expressions for the amplitudes  $u_N^{(\epsilon)}(n)$  and  $v_N^{(\epsilon)}(n)$  in (9) for generic and for dissipative QW codeword states.

#### 1. Generic QW codeword states

In the generic (unitary) case if the initial state is the horizontally polarized squeezed-vacuum state  $|0\rangle_r|H\rangle$ , one has after  $N$  steps of QWs for  $n \neq \pm N$  [26]

$$u_N^{(H)}(n) = \frac{1}{\sqrt{2^N}} \sum_{k=0}^{k_u} \binom{\frac{N-n-2}{2}}{k} \binom{\frac{N+n}{2}}{k+1} (-1)^{\frac{N-n}{2}-k-1},$$

$$v_N^{(H)}(n) = \frac{1}{\sqrt{2^N}} \sum_{k=0}^{k_v} \binom{\frac{N-n-2}{2}}{k} \binom{\frac{N+n}{2}}{k} (-1)^{\frac{N-n}{2}-k-1}, \quad (\text{A1})$$

where the upper bounds for the summations are

$$k_u \equiv \min \left\{ \frac{N-n-2}{2}, \frac{N+n-2}{2} \right\} \quad \text{and} \quad k_v \equiv \min \left\{ \frac{N-n-2}{2}, \frac{N+n}{2} \right\}. \quad (\text{A2})$$

For the boundary points  $n = \pm N$ , one finds

$$\begin{aligned} u_N^{(H)}(+N) &= \frac{1}{\sqrt{2^N}}, \quad u_N^{(H)}(-N) = 0, \\ v_N^{(H)}(+N) &= 0, \quad v_N^{(H)}(-N) = \frac{(-1)^{N-1}}{\sqrt{2^N}}. \end{aligned} \quad (\text{A3})$$

In the case of a vertically polarized squeezed-vacuum state  $|0\rangle_r|V\rangle$  initially, one finds after  $N$  steps of QWs for  $n \neq \pm N$

$$\begin{aligned} u_N^{(V)}(n) &= \frac{1}{\sqrt{2^N}} \sum_{k=0}^{k'_u} \binom{\frac{N+n-2}{2}}{k} \binom{\frac{N-n}{2}}{k} (-1)^{\frac{N-n}{2}-k}, \\ v_N^{(V)}(n) &= \frac{1}{\sqrt{2^N}} \sum_{k=0}^{k'_v} \binom{\frac{N+n-2}{2}}{k} \binom{\frac{N-n}{2}}{k+1} (-1)^{\frac{N-n}{2}-k-1}, \end{aligned} \quad (\text{A4})$$

where the upper bounds for the summations are

$$k'_u \equiv \min \left\{ \frac{N+n-2}{2}, \frac{N-n}{2} \right\} \quad \text{and} \quad k'_v \equiv \min \left\{ \frac{N+n-2}{2}, \frac{N-n-2}{2} \right\}. \quad (\text{A5})$$

For the boundary points  $n = \pm N$ , one gets

$$\begin{aligned} u_N^{(V)}(+N) &= \frac{1}{\sqrt{2^N}}, \quad u_N^{(V)}(-N) = 0, \\ v_N^{(V)}(+N) &= 0, \quad v_N^{(V)}(-N) = \frac{(-1)^N}{\sqrt{2^N}}. \end{aligned} \quad (\text{A6})$$

## 2. Dissipative QW codeword states

In the dissipative case, as pointed out in the text, the  $H$  and the  $V$  polarizations are now symmetric. Therefore, for both types of initial states  $|0\rangle_r|H\rangle$  and  $|0\rangle_r|V\rangle$ , one has the same result for the amplitudes after  $N$  steps of QWs. We can thus drop the superscripts  $(\epsilon)$  for polarizations in  $u_N^{(\epsilon)}$  and  $v_N^{(\epsilon)}$  here. For  $n \neq \pm N$  we find

$$u_N(n) = \frac{1}{2^N} \binom{N-1}{\frac{N+n-2}{2}}, \quad \text{and} \quad v_N(n) = \frac{1}{2^N} \binom{N-1}{\frac{N+n}{2}}. \quad (\text{A7})$$

For the boundary points  $n = \pm N$ , we have

$$\begin{aligned} u_N(+N) &= \frac{1}{2^N}, \quad u_N(-N) = 0, \\ v_N(+N) &= 0, \quad v_N(-N) = \frac{1}{2^N}. \end{aligned} \quad (\text{A8})$$

The amplitudes  $w_N(n)$  in (15) after the projection onto  $D$  polarization can then be obtained through (A7) and (A8).

## Appendix B: Calculation for $P_{\text{no error}}$

Here we explain briefly how  $P_{\text{no error}}$  are calculated for the data plotted in Fig. 4. It has been shown by Glancy and Knill in Ref. 29 that when the shift errors in the codewords are bounded, it is possible to repeatedly recover the corrupted qubits without Pauli errors. To find the corresponding probability, the codewords are projected onto the basis set  $\{|s, t\rangle\}$  that consists of the ideal GKP codeword  $|0\rangle_L$  in (1) shifted in both  $x$  and  $p$  [29]

$$|s, t\rangle \equiv \pi^{-\frac{1}{4}} \sum_{m=-\infty}^{\infty} e^{-2imt\sqrt{\pi}} |2m\sqrt{\pi} + s\rangle_x, \quad (\text{B1})$$

where  $-\sqrt{\pi} \leq s \leq \sqrt{\pi}$  and  $-\sqrt{\pi}/2 \leq t \leq \sqrt{\pi}/2$  due to the periodicity of the  $|0\rangle_L$  state. The probability density for a state  $|\psi\rangle$  to have shifts  $s$  and  $t$  relative to the ideal GKP codeword  $|0\rangle_L$  is then given by  $|\langle s, t|\psi\rangle|^2$ . As demonstrated

in Ref. [29], when the shift errors of a codeword are bounded within the range  $[-\sqrt{\pi}/6, +\sqrt{\pi}/6]$  for both  $x$  and  $p$  quadratures, it is then ensured that repeated error corrections will be successful. Namely, for the dQW codeword  $|0\rangle_{\text{dQW}}$ , the probability for repeated error corrections without incurring errors is

$$P_{\text{no error}} \equiv \int_{-\frac{\sqrt{\pi}}{6}}^{+\frac{\sqrt{\pi}}{6}} ds \int_{-\frac{\sqrt{\pi}}{6}}^{+\frac{\sqrt{\pi}}{6}} dt |\langle s, t | 0 \rangle_{\text{dQW}}|^2. \quad (\text{B2})$$

Following Eqs. (14)–(16) and (B1), one finds upon invoking (12) for  $\Delta x = \sqrt{\pi}$

$$\langle s, t | 0 \rangle_{\text{dQW}} = \left( \frac{e^{+r}}{\pi Z_N} \right)^{\frac{1}{2}} \sum_{m=-\infty}^{\infty} \sum_{n=-N}^N w_N(n) e^{+2imt\sqrt{\pi}} \exp \left[ -\frac{s + (2m - n)\sqrt{\pi}}{2e^{-2r}} \right]. \quad (\text{B3})$$

Substituting (B3) into (B2), one can obtain the results displayed in Fig. 4 accordingly.

---

[1] M. A. Nielsen and I. L. Chuang, *Quantum Computation and Quantum Information* (Cambridge University Press, Cambridge, 2000).

[2] Castelvecchi, Nature **541**, 9 (2017).

[3] D. A. Lidar and T. A. Brun (Eds.), *Quantum Error Correction* (Cambridge University Press, Cambridge, 2013).

[4] J. Zhang and S. L. Braunstein, Phys. Rev. A **73**, 032318 (2006).

[5] N. C. Menicucci, P. van Loock, M. Gu, C. Weedbrook, T. C. Ralph, and M. A. Nielsen, Phys. Rev. Lett. **97**, 110501 (2006).

[6] N. C. Menicucci, Phys. Rev. Lett. **112**, 120504 (2014).

[7] K. Fukui, A. Tomita, and A. Okamoto, Phys. Rev. Lett. **119**, 180507 (2017).

[8] K. Fukui, A. Tomita, A. Okamoto, and K. Fujii, Phys. Rev. X **8**, 021054 (2018).

[9] D. Gottesman, A. Kitaev, and J. Preskill, Phys. Rev. A **64**, 012310 (2001).

[10] B. C. Travaglione and G. J. Milburn, Phys. Rev. A **66**, 052322 (2002).

[11] S. Pirandola, S. Mancini, D. Vitali, and P. Tombesi, Europhys. Lett. **68**, 323 (2004).

[12] S. Pirandola, S. Mancini, D. Vitali, and P. Tombesi, Eur. Phys. J. D **37**, 283 (2006).

[13] S. Pirandola, S. Mancini, D. Vitali, and P. Tombesi, J. Phys. B **39**, 997 (2006).

[14] H. M. Vasconcelos, L. Sanz, and S. Glancy, Opt. Lett. **35**, 3261 (2010).

[15] P. Brooks, A. Kitaev, and J. Preskill, Phys. Rev. A **87**, 052306 (2013).

[16] B. M. Terhal and D. Weigand, Phys. Rev. A **93**, 012315 (2016).

[17] K. R. Motes, B. Q. Baragiola, A. Gilchrist, and N. C. Menicucci, Phys. Rev. A **95**, 053819 (2017).

[18] C. Fluhmann, T. L. Nguyen, M. Marinelli, V. Negnevitsky, K. Mehta, and J. Home, Preprint arXiv:1807.01033.

[19] J. Kempe, Contemp. Phys. **44**, 307 (2003).

[20] K. Manouchehri and J. Wang, *Physical Implementation of Quantum Walks* (Springer-Verlag, Berlin, 2014).

[21] S. L. Braunstein and A. K. Pati (Eds.), *Quantum Information with Continuous Variables* (Kluwer Academic, Dordrecht, 2003).

[22] S. L. Braunstein and P. van Loock, Rev. Mod. Phys. **77**, 513 (2005).

[23] A. Schreiber, K. N. Cassemiro, V. Potoček, A. Gábris, P. J. Mosley, E. Andersson, I. Jex, and Ch. Silberhorn, Phys. Rev. Lett. **104**, 050502 (2010).

[24] Here the extra factor  $\sqrt{2}$  comes from defining the Hermitian part of the mode operator  $\hat{a}$  to be  $\hat{x}/\sqrt{2}$  (and hence  $\hbar = 1$ ). If one instead uses  $\hat{x}$  for the Hermitian part of  $\hat{a}$  (thus  $\hbar = 1/2$ ), such factors of  $\sqrt{2}$  would disappear. Here we are following conventions used in the GKP literatures.

[25] A. Furusawa, J. L. Sørensen, S. L. Braunstein, C. A. Fuchs, H. J. Kimble, and E. S. Polzik, Science **282**, 706 (1998).

[26] A. Ambainis, E. Bach, A. Nayak, A. Vishwanath, and J. Watrous in *Proceedings of the 33rd Annual ACM Symposium on Theory of Computing* (Hersonissos, Greece, ACM New York, 2001), p. 37-49.

[27] A. Schreiber, A. Gábris, P. P. Rohde, K. Laiho, M. Stefanak, V. Potoček, C. Hamilton, I. Jex, and Ch. Silberhorn, Science **336**, 55 (2012).

[28] V. Kendon, Math. Struct. in Comp. Science **17**, 1169 (2007).

[29] S. Glancy and E. Knill, Phys. Rev. A **73**, 012325 (2006).

[30] H. Vahlbruch, M. Mehmet, K. Danzmann, and R. Schnabel, Phys. Rev. Lett. **117**, 110801 (2016).